IEEE Transactions on Components, Packaging, and Manufacturing Technology

Physics-based Analytical Engineering Models of Graphene Micro- and Nanostrip Lines

Journal:	*Transactions on Components, Packaging and Manufacturing Technology*
Manuscript ID	Draft
Manuscript topic:	TCPMT Paper
Date Submitted by the Author:	n/a
Complete List of Authors:	Kouzaev, Guennadi; Norwegian University of Science and Technology, Electronic Systems
Keywords:	graphene microstrip line, graphene nanostrip line, an analytical model

Physics-based Analytical Engineering Models of Graphene Micro- and Nanostrip Lines

Guennadi Kouzaev[1], *Member, IEEE*

***Abstract*—In this paper, new approximate analytical models of graphene-based micro-and nanostrip transmission lines are given. These models are based on the representation of the mentioned lines by a parallel-plate waveguide embedded into an effective frequency-dependent permittivity media. Our theory allows analytical calculation of complex propagation constant and characteristic impedance of the main quasi-TM mode of graphene strip transmission lines. The developed approach is verified by comparisons with the thin-film lossy microstrips, for which the measurements and theory are available for frequencies up to 1 THz and with parallel-plate graphene waveguides. For very-narrow lines, the developed model is improved by a correction tuning technique. The obtained analytical formulas for complex propagation constant and characteristic impedance are interesting for calculations of electronically controlled graphene-based interconnects, microwave and millimeter wave attenuators, antennas, and transistors.**

***Index Terms*— graphene microstrip line, graphene nanostrip line, an analytical model**

I. Introduction

GRAPHENE material [1] is interesting in the developments of new electronics and optoelectronics, including microwave and terahertz transistors [2]-[4]. An attractive feature of graphene components is their low signal delay and the possibility of tuning of their parameters using the electric or/and magnetic biasing of graphene's chemical potential and the conductivity of graphene layers [4],[5]. For instance, even loss of graphene interconnects can be decreased, tuning the chemical potential that is shown in measurements and simulations [6],[7]. Many linear and nonlinear graphene devices are published for analog microwave integrations [2],[4],[8],[9].

Similarly to that made for conventional electronics, the models of graphene components for computer-aided design (CAD) software tools should be created for the design system libraries [5]. The most analytically studied transmission line is the parallel-plate waveguide, where the graphene-one-atom layers are separated by a dielectric and biased by electric or/and magnetic fields [10]-[15]. Approximate analytical models for graphene microstrips are unknown, unlike conventional microstrips. There are some papers on numerical simulations using the integral equation method, technique of Fourier transform, method of lines, and the use of commercial software tools are published [5],[13]-[21]. Experimental results on graphene-based components are with electronically controlled antennas, attenuators, filters, field-effect transistors [4]. Some papers are on the measurements of graphene microstrip transmission lines [21]-[23].

Analytical calculation of microstrip interconnects [24],[25] encounters some difficulties caused by the known and still unsolved problems in the theory of printed transmission lines complicated by loss properties of scalar or anisotropic graphene layers.

In this paper, a new approximate analytical physics-based model of graphene microstrip proposed allowing to calculate the complex propagation constant and characteristic impedance.

II. Theoretical Model of a Graphene Microstrip Line

The cross-section of the modeled graphene microstrip line is shown in Fig. 1a.

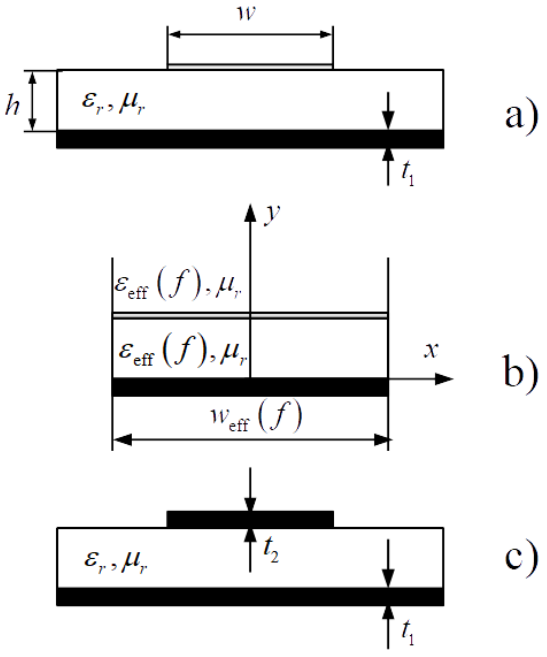

Fig. 1. Cross-sections of the studied integrated transmission lines. a) Graphene microstrip (nanostrip) line; b) Equivalent parallel plate model of graphene microstrip (nanostrip) line with the ideal magnetic walls placed at the effective width $w_{\text{eff}}(f)$ from each other; c) Thin-film microstrip line.

[1] Submitted on June 15, 2019. Author is with Norwegian University of Science and Technology-NTNU, Trondheim, No-7491, Norway. E-mail: guennadi.kouzaev@ntnu.no

The atomic-thick graphene signal strip conductor (in grey color) of the width w placed on the surface of the substrate of the relative permittivity ε_r, relative permeability $\mu_r = 1$, and the height h.

In general case, the graphene layer properties are anisotropic and described with a conductivity tensor $\underline{\underline{\sigma}}$ [18], [26]:

$$\underline{\underline{\sigma}} = \begin{pmatrix} \sigma_{11} & \sigma_{12} \\ \sigma_{21} & \sigma_{22} \end{pmatrix}. \quad (1)$$

Another side of this substrate is covered with a thin metal layer of the specific conductivity $\sigma_1^{(s)}$ and thickness t_1, or it can be assumed as a perfect conductor with $\sigma_1^{(s)} = \infty$.

The first theories of conventional microstrip lines relate to the beginning of the 50th of the last century when, firstly, the strip-line cross-section was transformed into a parallel plate geometry on a complex plane, and the potential, electric field, and characteristic impedance of the main transversal electromagnetic (TEM) mode were calculated. Microstrip lines have the layered dielectric design, and they can be calculated by the method of conformal mapping only in an approximate manner. For this purpose, the line is filled by an effective dielectric media uniformly, and again the same method allows to calculate the modal parameters. The hybrid nature of mode is considered by introducing the frequency-dependent effective permittivity. To analyze the microstrip discontinuities, the microstrips are represented by parallel-plate waveguide filled by the effective modal permittivity, and even multi-modal diffraction effects are described in this manner using the mathematical means or equivalent circuits of discontinuities [27].

Loss calculation in microstrips is a rather challenging problem, especially in a wide frequency band. Many models are known and used in engineering practice. One of them is our parallel-plate approximation validated by published measurement at frequencies up to 150 GHz, and by comparisons with some numerical simulations up to 1 THz [24],[25]. In this model, parallel-conductor plates are substituted by equivalent impedance walls, and no field is supposed outside the cross-section of this parallel-plate waveguide filled with an effective permittivity media and limed by magnetic walls placed at a certain effective distance w_{eff} from each other. The theory gives the complex propagation constant and characteristic impedance, and it is accurate for the wide thin-film conductor and electrically thin-substrate microstrips used in microwave integrated electronics.

Direct application of this model to graphene microstrip shows its inaccuracy because electromagnetic (EM) field penetrates the atomically thin graphene, and it is strong over this layer, and, at the difference to conventional conductors, this field should be considered when we are formulating a parallel-plate model of the graphene microstrip line.

The main idea of this contribution is that the parallel-plate geometry of the microstrip model is embedded into the uniform effective permittivity media (Fig. 2), and it allows to obtain analytical expressions for the complex modal propagation constant and characteristic impedance. Otherwise, placing this mentioned geometry into a layered media allows getting the dispersion equations solved only numerically regarding complex longitudinal propagation constant k_z.

Before to provide the EM treatment for this model (Fig. 2), let's consider the parameters of all components of this equivalent waveguide. It is supposed that it is filled with the effective frequency-dependent permittivity media $\varepsilon_{\text{eff}}(f)$ (see Appendix A for the calculation formulas), and it is of the effective frequency-depending width $w_{\text{eff}}(f)$.

Considering the anisotropic graphene and lossy ground conductor represented with its surface impedance, the field of the main mode in the parallel-plate waveguide (Fig. 1b) is hybrid, and it has all six field components. This field is written using two vector potential functions for each layer, supposing the independence of the field according to the $x-$ direction:

$$\mathbf{\Phi}^{(1,2)}(y,z) = \mathbf{y}_0 \Phi_y^{(1,2)}(y) e^{-jk_z z}, \quad (2)$$

$$\mathbf{\Psi}^{(1,2)}(y,z) = \mathbf{y}_0 \Psi_y^{(1,2)}(y) e^{-jk_z z} \quad (3)$$

where k_z is the unknown longitudinal propagation constant.

For our further treatment, we need only the fields $\mathbf{E}_\tau = \mathbf{x}_0 E_x + \mathbf{z}_0 E_z$ and $\mathbf{H}_\tau = \mathbf{x}_0 H_x + \mathbf{z}_0 H_z$, which are tangential to the plates of the waveguide (Fig. 1b):

$$\begin{aligned} E_x^{(1,2)}(y,z) &= jk_z \Psi_y^{(1,2)}(y) e^{-jk_z z}, \\ E_z^{(1,2)}(y,z) &= -\frac{k_z}{\omega \varepsilon_0 \varepsilon_{\text{eff}}(f)} \frac{\partial^2 \Phi_y^{(1,2)}(y)}{\partial y} e^{-jk_z z}, \\ H_x^{(1,2)}(y,z) &= jk_z \Phi_y^{(1,2)}(y) e^{-jk_z z}, \\ H_z^{(1,2)}(y,z) &= -\frac{k_z}{\omega \mu_0 \mu_r} \frac{\partial \Psi_y^{(1,2)}(y)}{\partial y} e^{-jk_z z} \end{aligned} \quad (4)$$

with

$$\begin{aligned} \Phi_y^{(1)}(y) &= \left(A \cos k_y y + B \sin k_y y\right), \\ \Psi_y^{(1)}(y) &= \left(C \cos k_y y + D \sin k_y y\right), \\ \Phi_y^{(2)}(y) &= E e^{-jk_y (y-h)}, \\ \Psi_y^{(2)}(y) &= F e^{-jk_y (y-h)} \end{aligned} \quad (5)$$

where $j = \sqrt{-1}$, ε_0 is the vacuum absolute permittivity, μ_0 and μ_r are the vacuum absolute and media's relative permeabilities, correspondingly, $k_y = \sqrt{k_0^2 \varepsilon_{\text{eff}}(f) \mu_r - k_z^2}$, $k_0 = \omega / c$, c is the light velocity in mm/s, and $\omega = 2\pi f$, and f is the driving frequency in Hertz. The constants A, B, C, D, E, F, and k_z are unknown, and they are obtained from the boundary conditions.

The first two of them are on the tangential to the boundary fields $\mathbf{E}_\tau^{(1)}(y=0)$ and $\mathbf{H}_\tau^{(1)}(y=0)$ matched at the surface of

the ground layer using the Leontovich's boundary condition that gives two equations:

$$\mathbf{E}_\tau^{(1)}(y=0)+Z_s^{(1)}\left[\mathbf{H}_\tau^{(1)}(y=0)\times\mathbf{n}_1\right]=0 \qquad (6)$$

where $Z_s^{(1)}$ is the surface impedance of the ground layer specified below in formula (13), $\mathbf{n}_1$ is the normal vector to the boundary 1 and oriented along the $y-$axis.

Other four boundary equations are written for the graphene layer supposing its zero thickness:

$$\begin{aligned}&\mathbf{E}_\tau^{(2)}(y=h)-\mathbf{E}_\tau^{(1)}(y=h)=0,\\&\mathbf{H}_\tau^{(2)}(y=h)-\mathbf{H}_\tau^{(1)}(y=h)=\underline{\sigma}_2\mathbf{E}_\tau^{(2)}(y=h)\end{aligned}. \qquad (7)$$

These boundary conditions (6) and (7) give the six linear algebraic equations regarding A, B, C, D, E, F. The determinant of this homogeneous system delivers a transcendental equation for the propagation constant k_z of the treated waveguide (Fig. 2) filled with $\varepsilon_{\text{eff}}(f)$ and being equivalent to the graphene microstrip line (Fig. 1a). This system order can be decreased down to four if the ground layer is considered being perfect.

A. *Anisotropic Graphene-Perfect Ground Layer Line*

In this case, the two potential functions for two layers are:

$$\begin{aligned}&\Phi_y^{(1)}(y)=B\cos k_y y,\\&\Psi_y^{(1)}(y)=D\sin k_y y,\\&\Phi_y^{(2)}(y)=Ee^{-jk_y(y-h)},\\&\Psi_y^{(2)}(y)=Fe^{-jk_y(y-h)}.\end{aligned} \qquad (8)$$

These functions provide the fields satisfying the boundary condition on the ideal metal; the other four equations are on the boundary with the graphene layer (see Equ. (7)). It gives the following eigenvalue equation regarding the longitudinal propagation constant k_z:

$$\det\begin{pmatrix}0 & \sin(k_y h) & 0 & -1\\ -\sin(k_y h) & 0 & j & 0\\ 0 & \dfrac{k_y\cos(k_y h)}{\omega\mu_0\mu_r} & \dfrac{-jk_y\sigma_{12}}{\omega\varepsilon_0\varepsilon_{eff}(f)} & \dfrac{k_y}{\omega\mu_0\mu_r}+j\sigma_{11}\\ -\cos(k_y h) & 0 & 1+\dfrac{\sigma_{22}k_y}{\omega\varepsilon_0\varepsilon_{eff}(f)} & -\sigma_{21}\end{pmatrix}=0 \qquad (9)$$

Supposing that the substrate is electrically thin, $|k_y h|\ll 1$, $\sin(k_y h)\approx k_y h$, $\cos(k_y h)\approx 1$, the analytical treatment of the determinant (9) gives:

$$k_y^2\frac{h\sigma_{22}}{k_0^2\varepsilon_{\text{eff}}(f)\mu_r}+k_y\frac{h(j-1)}{\omega\mu_0\mu_r}-\left(\sigma_{11}h+\frac{1}{\omega\mu_0\mu_r}\right)=0. \qquad (10)$$

This quadratic eigenvalue equation is solved regarding k_y analytically, and one of the roots corresponds to the quasi-TM main mode of the considered transmission line. It is seen that although σ_{12} and $\sigma_{2,1}$ are not seen in this formula, the influence of anisotropy of conductivity remains in hybrid nature of the main mode caused by this conductivity, and it needs to be considered in the theory of graphene microstrip line if its conductivity is anisotropic that is in correspondence to the conclusion of [18].

The longitudinal propagation constant k_z is derived immediately from $k_z=\sqrt{k_0\varepsilon_{\text{eff}}(f)\mu_r-k_y^2}$ choosing the needed branch of the imaginary part of this propagation constant properly.

For calculation of the characteristic impedance for the main mode, the boundary equations (6) and (7) should be solved if the propagation constant k_z is found from (9) or (10). Then, this parameter is found as a relationship between the graphene current and line voltage. An example of such formulas is shown below.

B. *Scalar Graphene-Imperfect Ground Layer Line*

Another important variant is the biasing of the graphene layer by only the electric field. At sub-Terahertz region, graphene, according to the opinions of many authors, can be described by scalar conductivity σ_2. Then, in the parallel-plate waveguide, the electric and magnetic types of modes can be classed independently regarding the $y-$axis [14],[15].

Consider the correspondence of these modes to the main mode of the graphene microstrip line. It is obvious that this mode should have a strong E_y component similarly to the conventional microstrip. Due to the loss in ground and graphene, the main mode should have the longitudinal component of the electric field, and this mode can be related to the quasi-TM modes [24],[25]. Then, to model this main mode of graphene microstrip, the E_y- lowest mode of equivalent the parallel plate waveguide is used for our further treatment. To describe this mode, the following potential functions are chosen:

$$\begin{aligned}&\Phi_y^{(1)}=A\cos k_y y+B\sin k_y y,\\&\Phi_y^{(2)}=Ce^{-jk_y(y-h)}.\end{aligned} \qquad (11)$$

Using (4) and (11) for only $\mathbf{\Phi}_e^{(1,2)}(y,z)$ and the boundary conditions (6) and (7), one can obtain the following eigenvalue equation for k_z:

$$\det\begin{pmatrix} -\cos(k_y h) & -\sin(k_y h) & 1-\dfrac{\sigma_2 k_y}{\omega\varepsilon_0\varepsilon_{\text{eff}}(f)} \\ -\sin(k_y h) & \cos k_y h & j \\ jZ_s^{(1)} & \dfrac{-k_y}{\omega\varepsilon_0\varepsilon_{\text{eff}}(f)} & 0 \end{pmatrix} = 0 \quad (12)$$

where

$$Z_s^{(1)} = -jZ_{0M}^{(1)}\cot(k_1 t_1), \quad (13)$$

$Z_{0M}^{(1)} = (1+j)\sqrt{\dfrac{\omega\mu_0\mu_r^{(1)}}{2\sigma_1^{(s)}}}$, and $k_1 = \dfrac{1-j}{\sqrt{\omega\mu_0\mu_r^{(1)}\sigma_1^{(s)}/2}}$,

$\mu_r^{(1)}$ is the conductor's relative permeability constant, $\sigma_1^{(s)}$ is the ground conductor's specific conductivity, and t_1 is the ground conductor thickness.

The scalar conductivity σ_2 of an isolated carbon sheet is calculated using one of the known approximate formulas, for instance, from [18]:

$$\sigma_2 = \frac{-je^2 k_B T}{\pi\hbar^2(\omega - j\tau^{-1})}\ln\left(2\left(1+\cosh\left(\frac{\mu_c(E_{\text{bias}})}{k_B T}\right)\right)\right), \quad (14)$$

which is valid for $k_B << |\mu_c|, \hbar\omega$. In this formula, e is the electron charge, k_B is the Boltzmann constant, T is the absolute temperature in Kelvin, $\hbar$ is the reduced Planck constant, τ is the scattering rate constant, m is the electron mass, and $\mu_c(E_{\text{bias}})$ is the graphene chemical potential that can be controlled applying the biasing electric field E_{bias}.

Supposing that the substrate is electrically thin and $|k_y h| \ll 1$, the analytical treatment of the determinant (12) gives

$$k_y^3\frac{\sigma_2 h}{(\omega\varepsilon_0\varepsilon_{\text{eff}}(f))^2} - k_y^2\frac{h}{\omega\varepsilon_0\varepsilon_{\text{eff}}(f)} + k_y\left(j\frac{1+\sigma_2 Z_s^{(1)}}{\omega\varepsilon_0\varepsilon_{\text{eff}}(f)} + hZ_s^{(1)}\right) - jZ_s^{(1)} = 0. \quad (15)$$

Analysis of this equation shows that the conductivity parameter σ_2 is a coefficient multiplying the cubic term. It means that solution may be highly sensitive towards the inaccuracy of graphene conductivity model. An additional means of accuracy control is the calculation of the determinant (12) at the root found with (15).

This cubic equation is solved analytically with the Cardano's formulas [28]. If k_y is found, the longitudinal propagation constant k_z is derived immediately from $k_z = \sqrt{k_0\varepsilon_{\text{eff}}(f)\mu_r - k_y^2}$ choosing the needed branch of the imaginary part of this propagation constant properly.

In *Matlab*, the roots of the cubic equation are derived using the function *roots*, and it gives three values of complex k_y. The first two of them are equal, and they are the sought mode transversal propagation constant k_y. The third complex root is small in its value, and it gives the longitudinal propagation constant k_z with $\text{Re}(k_z) \approx k_0\sqrt{\varepsilon_{eff}(f)\mu_r}$ and the negligibly small imaginary part of this constant.

If the boundary equation problem has been solved, the characteristic impedance for this mode is obtained as:

$$Z_c = \frac{U}{I} = \frac{\int_0^h E_y^{(1)}(y)dy}{\int_0^w \left(H_x^{(2)}(y=h) - H_x^{(1)}(y=h)\right)dx} = \frac{\int_0^h E_y^{(1)}(y)dy}{\sigma_2\int_0^{w_{\text{eff}}} E_z^{(2)}(y=h)dx} \quad (16)$$

with

$$E_y^{(2)}(y) = \frac{-jk_z^2}{\omega\varepsilon_0\varepsilon_{\text{eff}}(f)}\Phi_y^{(1)}(y), \qquad E_z^{(2)}(y) = \frac{jk_z}{\omega\varepsilon_0\varepsilon_{\text{eff}}(f)}\frac{d\Phi_y^{(2)}}{dy}. \quad (17)$$

As seen from (15), the calculation of complex propagation constant k_z in wide frequency band requires the formulas for loss-less microstrip line that take into account the frequency dependence of the effective permittivity $\varepsilon_{\text{eff}}(f)$ and the effective strip width $w_{\text{eff}}(f)$. In Appendix A, these engineering formulas are chosen considering many published papers according to the Author's experience and comparisons with the available numerical and experimental data.

III. Verification of the Developed Model

A. Comparisons with the Thin-film Lossy Microstrip Line Full-wave, Analytical, and Measurement Results

Equ. (15) is obtained for infinitely thin graphene strips embedded into uniform effective dielectric media. This technique has not been known before, and it should be tested. For instance, it can be verified with the results known for thin-film microstrips [24],[25],[29],[30]. Before to compare, the correspondence infinitely thin resistive microstrip model should be found to the thin-film ones. For this purpose, the conductivity σ_2 is calculated from the specific conductivity of signal conductors of testing microstrips as $\sigma_2 = \sigma_s^{(2)} t_2$ where t_2 is the conductor thickness.

The comparisons are shown in Figs 2-6 obtained for microstrips with $w/h = 4.7$ and 2.74. The ground layer is lossy for all calculations, and it is modeled according (13). For these thin film microstrips, the experimental, full-wave and analytical results are given at frequencies up to 1 THz.

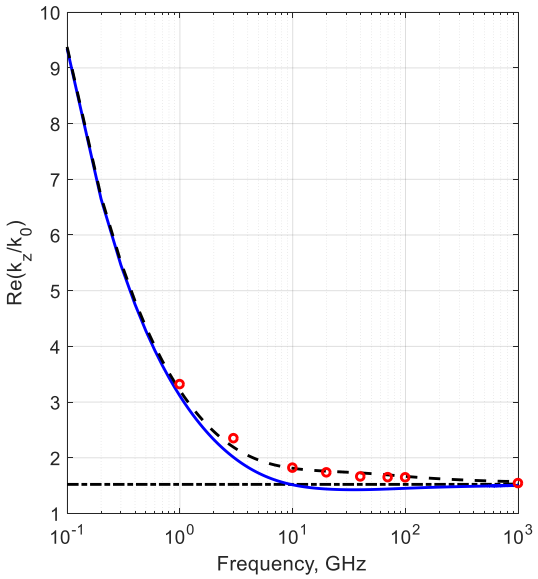

Fig. 2. The real part of k_z versus frequency. Solid violet line: formula (15); dash-dot black line: ideal conductor microstrip [31],[32],[33]; dash black line: thin-film microstrip analytical model [24],[25], and Appendix B; red circles: full-wave from [29]. Microstrip data: $\varepsilon_r = 2.7$, $\mu_r = 1$, $\tan\delta = 0.015$, $h = 1.7$ μm, $w = 8$ μm, $t_1 = t_2 = 0.8$ μm, $\sigma_1^{(s)} = \sigma_2^{(s)} = 2.5 \cdot 10^4$ Sim$\cdot$mm^{-1} .

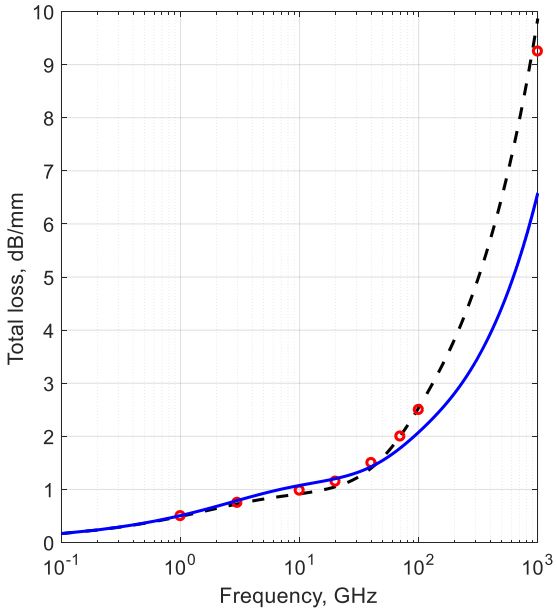

Fig. 3. Microstrip total (conductor+dielectric) loss α_t versus frequency. Solid violet line: formula (15); dash black line: thin-film microstrip analytical model [24],[25], and Appendix B; red circles: full-wave data from [28]. Microstrip data: $\varepsilon_r = 2.7$, $\mu_r = 1$, $\tan\delta = 0.015$, $h = 1.7$ μm, $w = 8$ μm, $t_1 = t_2 = 0.8$ μm, $\sigma_1^{(s)} = \sigma_2^{(s)} = 2.5 \cdot 10^4$ Sim$\cdot$mm^{-1}.

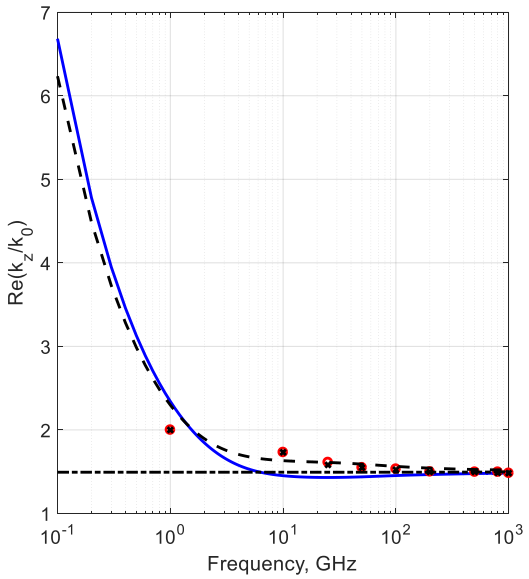

Fig. 4. The real part of k_z versus frequency. Solid violet line: formula (15); dash-dot black line: ideal conductor microstrip calculated according to [30],[31],[32]; dash black line: thin-film microstrip analytical model [24],[25], and Appendix B; red circles: numerical data from [30]; crosses: measurements from [30]. Microstrip data: $\varepsilon_r = 2.7$, $\mu_r = 1$, $\tan\delta = 0.015$, $h = 2.7$ μm, $w = 7.4$ μm, $t_1 = t_2 = 0.8$ μm, $\sigma_1^{(s)} = \sigma_2^{(s)} = 3 \cdot 10^4$ Sim$\cdot$mm^{-1} .

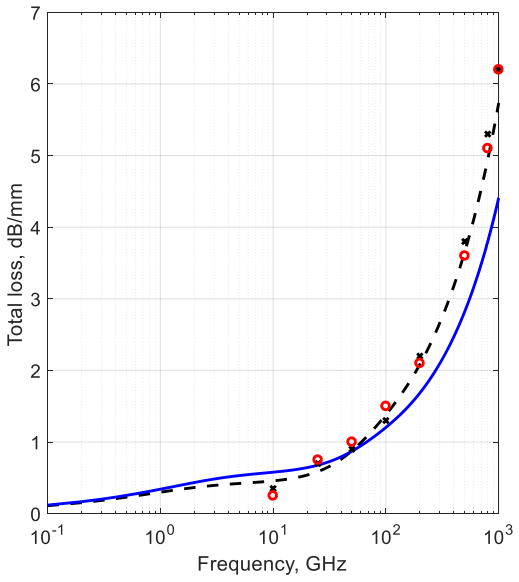

Fig. 5. Microstrip total (conductor+dielectric) loss α_t versus frequency. Solid violet line: formula (15); dash black line: thin-film microstrip analytical model [24],[25], and Appendix B; red circles: full-wave data from [30]; crosses: experimental from [29]. Microstrip data: $\varepsilon_r = 2.7$, $\mu_r = 1$, $\tan\delta = 0.015$, $h = 2.7$ μm, $w = 7.4$ μm, $t_1 = t_2 = 0.8$ μm, $\sigma_1^{(s)} = \sigma_2^{(s)} = 3 \cdot 10^4$ Sim$\cdot$mm^{-1} .

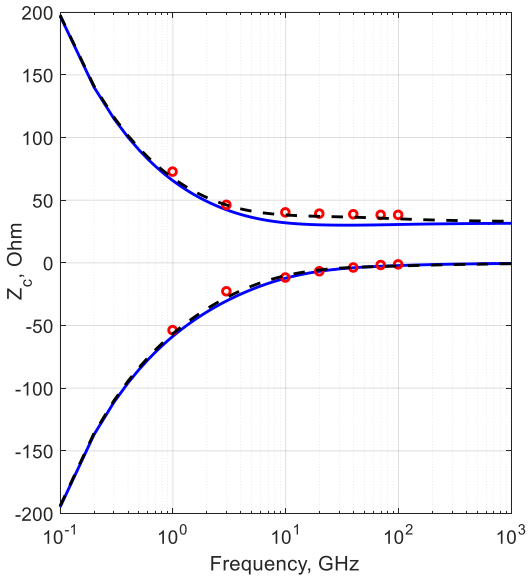

Fig. 6. The complex characteristic impedance of thin-film microstrip line versus frequency. Positive values are for the real part, and negative ones are for the imaginary part. Solid violet line: formula (16); dash black line: the approximate model of thin-film microstrip from [24],[25]; Red circles: full-wave results from [29]. Microstrip data are the same as at Figs. 3 and 4.

It is seen that the zero-thickness analytical model calculates the phase constant of the main mode and its characteristic impedance with good accuracy in the large frequency range comparing the full-wave, experimental, and approximate analytical results.

The loss is computed with less accuracy especially at frequencies over 100 GHz, and its reason is obvious. The thickness of all conductors and the skin effect must be taken into account in such thin-film microstrips. In the case of graphene lines with the atomically-thin signal conductor, this effect is expected to disappear, and this wide strip graphene lines should be calculated with good accuracy.

B. Modeling of Wide Graphene Microstrips and Comparisons with the Parallel-plate Analytical Results

The ultimate case of a wide-strip line is the parallel-plate waveguide treated analytically in many papers [5],[10],[12],[14],[17]. In [10], an analytical formula is given for a parallel-plate graphene line (see [10], p. 2, formula (15)). It is obtained under the assumptions $\left|k_y h\right| \ll 1$ and $\left|\sigma k_y / \omega\varepsilon_0\varepsilon_r\right| \gg 1$. Its both plates made of graphene layers, but this formula is pertinent to calculate the odd TEM mode of this waveguide. In this case, the cross-section of this line can be separated by an ideal electric wall. Our model can calculate this geometry as well, and the analytical results of G.W. Hanson compared with our simulation of a very wide $(w/h = 8)$ air-filled strip line. The results (Fig. 7) are close to each other at increased frequencies, but different at low ones because our theory is free of the restriction $\left|\sigma k_y / \omega\varepsilon_0\varepsilon_r\right| \gg 1$.

As seen from our simulations and published parallel-plate modeling, the graphene line has a rather strong loss at low-frequency microwaves. This loss is decreased with frequency

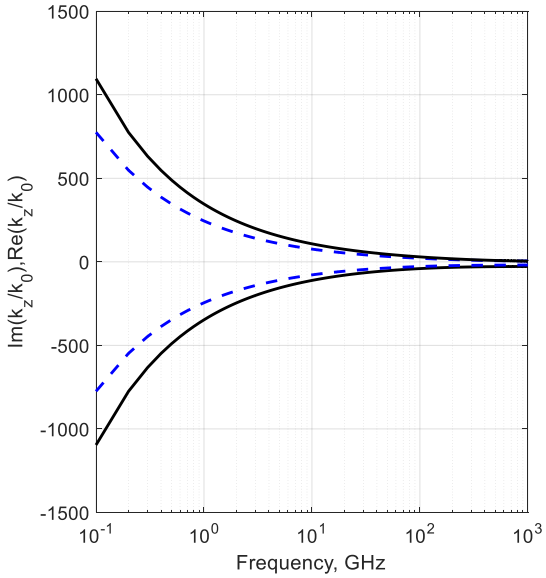

Fig. 7. The imaginary and real part of propagation constants versus frequency. Solid black lines: analytical results according to Hanson's formula; dash violet line: our results. The waveguide geometry and graphene's data: $h =$ 0.5 μm, $w = 20$ μm, $\varepsilon_r = 1, \mu_r = 1$, $\tan\delta = 0$, $\mu_c = 0$, $\tau = 0.5$ ps, $T = 300$ K.

and with the chemical potential controlled by the electric DC field.

Figs. 8, 9 shows the complex propagation constant and characteristic impedance for two values μ_c. It is seen that growing this parameter leads to the loss decrease compared with those brought by imperfect ground (Fig. 8). At the same time, it allows tuning the characteristic impedance to the values typical for conventional microstrips (Fig. 9) at the difference to the lines based on carbon nanotubes.

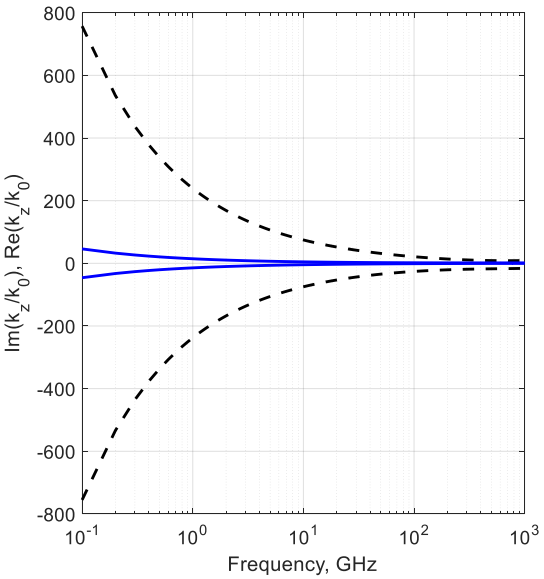

Fig. 8. Normalized complex propagation constant of microstrip line versus frequency. Positive values are for the real part, and the negative one is for the

imaginary part. Dash black line $\mu_c = 0$ eV; solid blue line $\mu_c = 10$ eV. Other parameters: $T = 300$ K, $\tau = 0.5$ ps, $\varepsilon_r = 3.9, \mu_r = 1$, $\tan\delta = 0$, $h = 1.7$ μm, $w = 8$ μm, $t_1 = 0.8$ μm, $\sigma_1^{(s)} = 2.5 \cdot 10^4$ Sim·mm^{-1}.

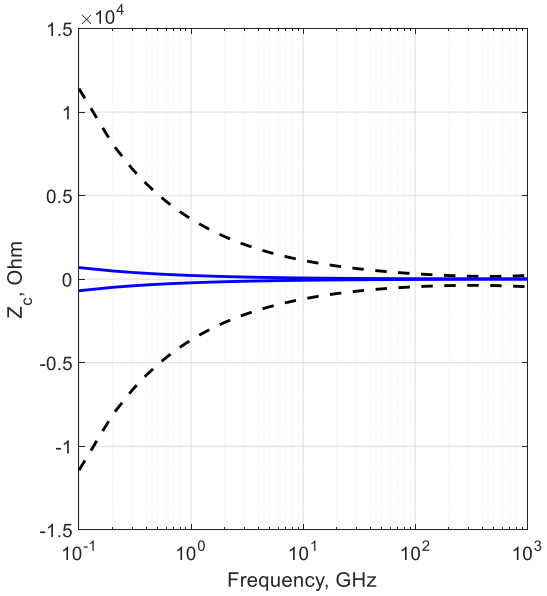

Fig. 9. Complex characteristic impedance versus frequency. Positive values are for the real part, and the negative one is for the imaginary part. Dash black line $\mu_c = 0$ eV; solid blue line $\mu_c = 10$ eV. $\mathrm{Re}(Z_c) \approx 50$ Ohm is at 20.7 GHz for $\mu_c = 10$ eV. Other parameters of microstrip and graphene are the same as at Fig. 8.

On Fig. 10, it is shown the S-matrix element dependence of a short length $(L = 1\,\mathrm{mm})$ of a graphene microstrip joined to 50-Ω ports.

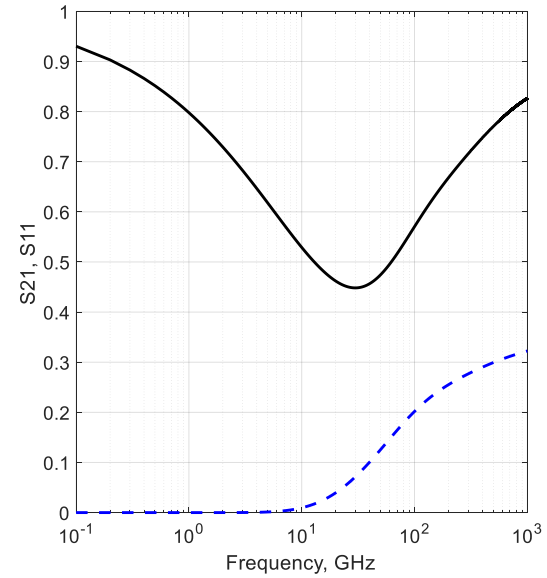

Fig. 10. The dependence of modules of the transmission (S21) and reflection (S11) coefficients of a length of the graphene transmission line. Parameters of microstrip and graphene conductors are the same as at Fig. 9.

It is seen that the reflection coefficient minimum occurs at a frequency near 30 GHz if the real impedance part of graphene microstrip characteristic impedance is tuned to 50-Ω at 20.7 GHz.

C. Comparisons with the Full-wave Simulations of the Narrow Graphene Micro- and Nanostrip Lines

The available in the literature full-wave results are for narrow-width $(w/h < 2-3)$ microstrip graphene lines which are difficult to be modeled by the equivalent parallel-plate approach. Usually, it is improved using the correction factors as in [24],[25]. The reason is that the ideal microstrip is modeled with the effective permittivity model. If the conductors have loss their conductivity should be substituted by its effective value one. Such models are not available, and up to now, the conductivity of conductor-surface impedances have been corrected empirically matching the models to the full-wave or measurement results. Physically, the currents in narrow strips are seriously distorted by edges and current-crowding effect, and the resistance of strips increases. The nonuniform distribution of current on the ground conductor can be taken as well [34]. To compensate it, the equivalent conductance of strip should be introduced. In practical modeling, the conductance of the strip can be reduced using the empirically found coefficients similarly to [24],[25].

To test our model, a very narrow $(w/h = 0.2)$ nanostrip is chosen as the worst-case scenario for our approach. This line is simulated using the integral equation method in [18]. As expected, our model provides the rather large difference, especially at frequencies below 100 GHz for the real (Fig. 11) and imaginary (Fig. 12) parts of propagation constant, and the equivalent parallel-plate model in the case of narrow strips should be corrected.

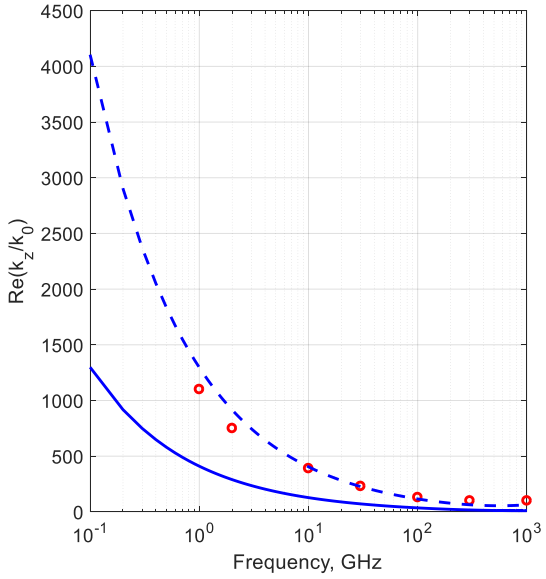

Fig. 11. The real part of normalized propagation constant versus frequency. Solid violet line: analytical calculations according (15). Red circles: simulations taken from [18] with graphical accuracy. Dash violet line: calculations with corrected graphene conductivity $(K_s = 0.1)$. Microstrip parameters:

$\varepsilon_r = 3.9, \mu_r = 1, \mu_r = 1, \tan\delta = 0, h = 0.5$ μm, $w = 100$ nm, $T = 300$ K, $\tau = 0.5$ ps, $\mu_c = 0$, $\sigma_1^{(s)} = \infty$, and σ_2 is calculated according (14).

The correction approach is chosen according to the above-described mechanism of the influence of non-uniformity of the current distribution along the strip width. By introducing the equivalent strip conductivity and correction of its value by $K_s = 0.1$, it is allowed to tune the results close to the full-wave calculations (Figs. 11 and 12). Of course, to make a complete tuning technique, there are more full-wave results needed to be obtained for a variety of microstrip geometries and physical parameters.

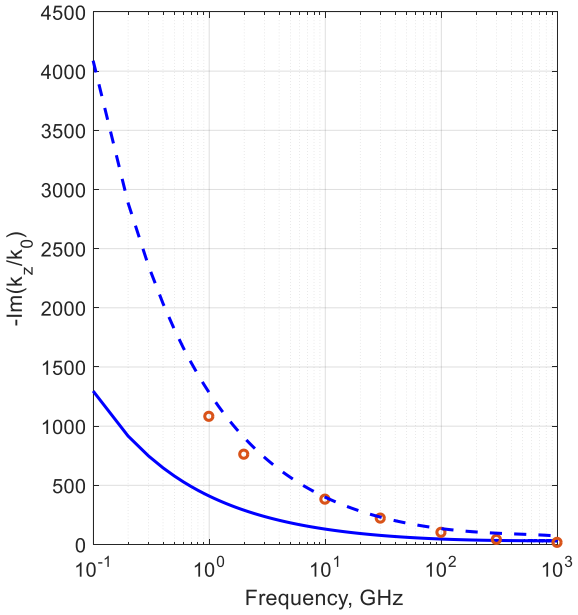

Fig. 12. The imaginary part of normalized propagation constant versus frequency. Solid violet line: analytical calculations according (15). Dash violet line: calculations with corrected graphene conductivity $(K_s = 0.1)$; Red circles: full-wave simulations taken from [18] with graphical accuracy. Microstrip parameters: $\varepsilon_r = 3.9$, $\mu_r = 1$, $\tan\delta = 0$, $h = 0.5$ μm, $w = 100$ nm, $T = 300$ K, $\tau = 0.5$ ps, $\mu_c = 0$, $\sigma_1^{(s)} = \infty$, and σ_2 is calculated according (14).

Because of the approximate nature of our modeling approach, it has some other limitations. For instance, the trigonometrical functions are represented by only first terms in their expansions considering the smallness of their arguments $|k_y h| \ll 1$. Accuracy can be increased considering more terms in analytical formulas if such solutions are available, or the equations (9) and (12) should be used.

The formula (15) is obtained considering the quasi-TM mode approximation. At increased frequencies, the six-field-component theory should be used. The skin effect models of the ground conventional conductors should be reconsidered as well using the Drude model of metals, for instance. Dielectric parameters would be better taken from the measurements at terahertz frequencies. For graphene applications, a conductivity theory of graphene placed on the surface of dielectrics is highly required. Otherwise, the conductivity parameters should be obtained from the measurements and populated for specified manufacturing technology.

IV. Conclusion

The approximate analytical formulas for complex propagation constant of graphene thin-substrate micro- and nanostrip transmission lines have been obtained, analyzed, and simulated. The first one is given for the tensor-conductivity graphene strips and ideal ground, and the second one is for "scalar" strip and imperfect ground layer. It has been shown that at the frequencies, where the strip conductivity is anisotropic, even the thin substrate microstrips are influenced by this anisotropy, and it needs to be modeled using the hybrid representation of EM field. Scalar conductivity micro- and nanostrip lossy lines, for which the full-wave and measurement results are available in the literature, have been modeled using the obtained analytical formulas, and good correspondence has been found in comparisons up 1 THz for wide-strip lines. It has been proposed to obtain the engineering formulas with empirically found correction factors for the narrow-strip graphene lines using the full-wave and measurement results. The obtained results can be used in practical calculations of graphene and lossy thin-film micro- and nanostrip lines, and as a means for the initial approximation of complex roots of eigenequations in full-wave computations.

V. Appendix A

To calculate the graphene microstrip line with above-given formulas, the ideal microstrip line parameters are needed. Ones of them are given in [33], and they are verified up to 1 THz comparing the numerical full-wave results from [29].

Considering that $k_z = \beta$, then, for an ideal microstrip

$$\sqrt{\varepsilon_{\text{eff}}(f)} = \frac{\beta}{k_0} = \frac{\sqrt{\varepsilon_r} - \sqrt{\varepsilon_{\text{eff}}}}{1 + 4F^{-1.5}} + \sqrt{\varepsilon_{\text{eff}}} \qquad (18)$$

where

$F = \dfrac{4hc\sqrt{\varepsilon_r - 1}}{f}\left[0.5 + \left\{1 + 2\cdot\lg\left(1 + \dfrac{w}{h}\right)\right\}^2\right]$, and ε_{eff} is the quasi-static effective permittivity of the microstrip line. This quasi-static permittivity is calculated according to the well-known engineering formulas [31].

$$\varepsilon_{\text{eff}} = \frac{\varepsilon_r + 1}{2} + \frac{\varepsilon_r - 1}{2}\left(1 + \frac{10}{u}\right)^{-ab} \qquad (19)$$

where

$$u = w/h,\ a = 1 + \frac{1}{49}\log\frac{u^4 + (u/52)^2}{u^4 + 0.432} + \frac{1}{18.7}\log\left[1 + \left(\frac{1}{18.1}\right)^3\right],$$

$$b = 0.564\left(\frac{\varepsilon_r - 0.9}{\varepsilon_r + 3}\right)^{0.053} .$$

The characteristic impedance calculations require the frequency-dependent effective width $w_{\text{eff}}(f)$ [25],[31]

$$w_{\text{eff}}(f) = w + (w_{\text{eff}} - w)\left[1 + \left(\frac{f}{f_c}\right)^2\right]^{-1} \quad \text{where} \qquad (20)$$

$$w_{\text{eff}} = \frac{120\pi h}{\sqrt{\varepsilon_{\text{eff}}} Z_c},\ f_c = c\Big/\left(2w_{\text{eff}}\sqrt{\varepsilon_{\text{eff}}}\right),\ Z_c = \frac{60}{\sqrt{\varepsilon_{\text{eff}}}}\log\left[\frac{p}{u} + \sqrt{1 + \left(\frac{2}{u}\right)^2}\right],$$

$$p = 6 + (2\pi - 6)\exp\left[-\left(\frac{30.666}{u}\right)^{0.7528}\right].$$

In (20), the thickness of the one-atom graphene strip layer is ignored.

VI. Appendix B

Approximate analytical formulas for calculation of complex propagation constant k_z and characteristic impedance Z_c of the main mode in thin-film microstrip lines are proposed and verified with measurements and full-wave simulations in [24] and [25]. For the convenience of Readers, it is shown below.

$$k_z^2 \approx k_0^2\varepsilon_{\text{eff}}(f) - \left(Z_s^{(1)} + K\cdot Z_s^{(2)}\right)\frac{j\omega\varepsilon_0\varepsilon_{\text{eff}}(f)}{h} + Z_s^{(1)}(K\cdot Z_s^{(2)})\left(j\omega\varepsilon_0\varepsilon_{\text{eff}}(f)\right)^2 \qquad (21)$$

where $Z_s^{(1,2)}$ is the surface impedance of conductors calculated according (13). The correction coefficient K is defined for narrow microstrip lines:

$$K = \begin{cases} 1, & w/h > 3...4 \\ 0.72, & w/h < 3...4 \end{cases} . \qquad (22)$$

The frequency dependent effective permittivity $\varepsilon_{\text{eff}}(f)$ is with formulas from Appendix A. The dielectric loss α_d is calculated using formulas of M.V. Schneider [32]:

$$\alpha_d = 27.3\frac{\varepsilon_r}{\varepsilon_r + 1}\frac{\varepsilon_{\text{eff}}(f) - 1}{\sqrt{\varepsilon_{\text{eff}}(f)}}\frac{\tan\delta}{\lambda_0[\text{mm}]},\ [\text{dB/mm}] \qquad (23)$$

where λ_0 is the wavelength in vacuum. The conductor loss α_c is derived as

$$\alpha_c = -10\lg\left(\exp\left(-2\cdot\text{Im}\left(k_z\cdot(l = 1\text{ mm})\right)\right)\right),\ [\text{dB/mm}]. \qquad (24)$$

The total loss α_t is a sum of these partial losses.

References

[1] A.K. Geim, and K.S. Novoselov, "The rise of graphene," *Nature Mat*., vol. 6, pp. 183-191, 2007.

[2] K.C. Ying, W.M. Wu, M.P. Pierpoint, and F.V. Kusmartsev, "Introduction to graphene electronics – a new era of digital transistors and devices," *Contemporary Phys*., vol. 54, pp. 233-251, 2013.

[3] J.S. Friedman, A. Girdhar, R.M. Gelfand, G. Memik, H. Mohseni, A. Taflove, B.W. Wessels, J.-P. Leburton, A.V Sahakian, "Cascaded spintronic logic with low-dimensional carbon," *Nature Commun*., vol. 8, pp. 1-7, 2017.

[4] M. Bozzi, L. Pierantoni, and S. Bellucci, "Applications of graphene at microwave frequencies," *Radioeng.*, vol. 24, pp. 661-669, 2015.

[5] M.B. Heydari, M.H.V. Samiei, "Plasmonic graphene waveguides: A literature review," *arXiv:1809.09937*, 27 p., 2018.

[6] Y. Wu, M. Qu, and Y. Liu, "A generalized lossy transmission-line model for tunable graphene-based transmission lines with attenuation phenomenon," *Sci. Rep*., vol. 6, pp. 31670, 2016.

[7] X. Zhou, T Zhang, L. Chen, W. Hong, and X. Li, "A graphene-based hybrid plasmonic waveguide with ultra-deep subwavelength confinement," *J. Lightwave Techn*., vol. 32, pp. 4199-4203.

[8] G.S. Makeeva, O.A. Golovanov, and G.A. Kouzaev, "Numerical analysis of tunable parametric terahertz devices based on graphene nanostructures using the projection method and autonomous blocks," *AIP Conf. Proc*., vol. 863, pp. 390003, 2017.

[9] G.S. Makeeva and O.A. Golovanov, *Mathematical Modelling of Terahertz-range Electronic-controlled Devices Based on Graphene and Nanocarbon Tubes* (in Russian), Penza State University Publ., 2018.

[10] G.W. Hanson, "Quasi-transverse electromagnetic modes supported by a graphene parallel-plate waveguide," *J. Appl. Phys*., vol. 104, pp. 084314, 2008.

[11] R. Araneo, G. Lovat, and P. Burghignoli, "Dispersion analysis of graphene nanostrip lines," *Proc. 2012 IEEE Int. Symp. Antennas. Propag*., pp. 75-78, 2012.

[12] A. Malekabadi, S.A. Charliebs, and D. Deslandes, "Parallel plate waveguide with anisotropic graphene plates: Effect of electric and magnetic biasing," *J. Appl. Phys*., vol. 113, pp. 113708 (1-9), 2013.

[13] A. Mehrdadian, H.H. Ardakani, and K. Forooraghi, "Analysis of two-dimensional graphene-based multilayered structures using the extended method of lines," *IEEE Access*, vol. 6, pp. 31503-31515, 2018.

[14] G. Lovat, P. Burghignoli, and R. Araneo, "Low-frequency dominant-mode propagation in spatially dispersive graphene nanowaveguides," *IEEE Trans. Electromag. Compat*., vol. 55, pp. 328-333, 2013.

[15] D. Correas-Serrano, J.S. Gomez-Diaz, J. Perruisseau-Carrier, and. A. Alvarez-Melcon, "Spatially dispersive graphene single and parallel plate waveguides: analysis and circuit model," *IEEE Trans., Microw. Theory Techn.*, vol. 61, pp. 4333-4344, 2013.

[16] K. Qin, R. Xiao, and R. Sun, "Mode analysis and research on graphene nanoribbons parallel-plate waveguide," *Micro&Nano Letters*, vol. 10, pp. 558-560, 2015.

[17] Y. Shao, J.J. Yang, and M. Huang, "A review of computational electromagnetic methods for graphene modeling," *Int. J. Anten. Propag*., vol. 2016, Art. 7478621, 2016.

[18] G. Lovat, G.W. Hanson, R. Araneo, and P. Burghignoli, "Comparison of spatially dispersive models for dyadic intraband conductivity of graphene," *Proc. 7th Eur. Conf. Anten. Propagat. (EUCAP 2013)*, pp. 500-504, 2013.

[19] H.H. Ardakani, Z.G. Kashani, M.K. Amirkalaee, and J. Rashed-Mohassei, "Fourier transform analysis of graphene-based multilayer structures," *IET Microw. Antennas&Propagat*., vol. 7, pp. 1084-1091, 2013.

[20] G. Lovat, D. Yi, P. Burghignoli, R. Araneo, S. Celozzi, and X.-C. Wei, "Theoretical study of the first higher-order mode in grounded graphene nanoribbons," *IEEE Trans., Nanotech*., vol. 17, pp. 814-823, 2018.

[21] S. Asif, A. Iftikhar, S.Z. Sajal, B. Braaten, and M.S. Khan, "On using graphene-based conductors as transmission lines for feed networks in printed antenna arrays," *Proc. 2015 IEEE Int. Conf. Electro/Information Technology*, pp. 681-683, 2015.

[22] K. Patel and K. Sharma, "Application of RLGC modeling in probing the electrical properties of monolayer graphene at microwave frequencies," *J. Electromag. Waves Appl*., vol. 32, pp. 1889-1897, 2018.

[23] O. Sanusi, P. Savi, S. Quaranta, A. Bayat, and L. Roy, " Equivalent circuit modeling of graphene-loaded thick films using S-parameters," *PIER Lett.*, vol. 76, pp. 33-38, 2018.

[24] G.A. Kouzaev, M.J. Deen, N.K. Nikolova, "A parallel-plate waveguide model of lossy microstrip lines," *IEEE Microw. Wireless Comp. Lett*., vol. 15, pp. 27-29, 2005.

[25] G.A. Kouzaev, *Applications of Advanced Electromagnetics. Components and Systems*. Heidelberg: Springer, 2013.

[26] G.W. Hanson, "Dyadic Green's function for an anisotropic, non-local model of biased graphene," *IEEE Trans., Antennas and Propagat.*, vol. 56, pp. 747-757.

[27] G. Kompa, *Handbook of Microwave Integrated Circuits*, Artech House, 2005.

[28] G.A. Korn and T.M. Korn, *Mathematical Handbook for Scientists and Engineers: Definitions, Theorems, and Formulas for Reference and Review*, Dover Publ., 2000.

[29] F. Schnieder and W. Heinrich, "Model of thin-film microstrip line for circuit design," *IEEE Trans., Microw. Theory Techn.*, vol. 49, pp. 104-110, 2001.

[30] F. Schnieder and W. Heinrich, "Thin-film microstrip lines and coplanar waveguides on semiconductor substrates for sub-mm wave frequencies," *Frequenz*, vol. 59, pp. 137-140, 2005.

[31] E. Hammerstad and O. Jensen, "Accurate models for microstrip computer-aided design," *IEEE MTT-S Int. Symp. Dig.*, 1980, pp. 407-409, 1980.

[32] M.V. Schneider. "Microstrip lines for integrated microwave circuits," *Bell Syst. Tech. J.*, vol. 48, pp. 1421-1444, 1969.

[33] E. Yamashita, K. Atsuki, and T. Hirahata, "Microstrip dispersion in a wide-frequency range," *IEEE Trans., Microw. Theory Techn.*, vol. 29, pp. 610-611, 1981.

[34] J.C. Liou and K.M. Lau, "Analysis of slow-wave transmission lines on multi-layered semiconductor structures including conductor loss," *IEEE Trans., Microw. Theory Techn.*, vol. 41, pp. 824-829, 1984.

Guennadi A. Kouzaev (M'2005) received the Ph.D. degree in Physics and Mathematics from the Kotelnikov's Institute of Radio Engineering and Electronics, USSR Academy of Sciences, Moscow, in 1986. He also has a Doctor of Sciences degree (1998) in Electrical Engineering from the Moscow State Institute of Electronics and Mathematics (Technical University)-MSIEM(TU), which is now a branch of the Higher School of Economics. From 1984 to 1989, he was with the Research Institute of Space Instrument Design, Moscow. From 1989 to 2000, he was with the MSIEM(TU). In 1993, he became an Associate Professor and, in 1999, a Full Professor with the MSIEM(TU). From 2000 to 2001, he was with Gennum Corp., Canada. From 2001 to 2005, he was with McMaster University, Canada. Currently, he is a Professor at the Department of Electronic Systems of Norwegian University of Science and Technology-NTNU, Trondheim, Norway. He is the author of one Springer book and an author of more than 200 papers, conference abstracts, and invention certificates. His current research interests are in electromagnetics and microwave techniques, applied quantum physics, microwave liquid heating, molecular dynamics in the electromagnetic field, and computers. He was a recipient of a 1997 Russian Government Prize for his contribution to the development and modeling of 3-D components for digital space-time modulated EM signals and computing circuits, and a 1990 Soviet Union Prize for Young Scientists for his contribution to the EM modeling and development of microwave 3-D circuits.